Chapter II

Experimental

This chapter describes the methodology to synthesize the TiO_2 and Mn doped TiO_2 nanoparticles, deposition of TiO_2 thin films, fabrication of pellets of TiO_2 with cement, post deposition effect on TiO_2 thin films by irradiating with low energy ion beam and discussed the experimental techniques used to characterize the synthesized samples as well as photocatalysis technique. Synthesis of TiO_2 and $Ti_{1-x}Mn_xO_2$ nanoparticles are given in Section 2.1. Section 2.2 describes thin film deposition by e-beam evaporation technique. Fabrication of TiO_2 and cement pellets are discussed in Section 2.3. A brief description of the ion irradiation technique is appended in Section 2.4. In Section 2.5 different characterization techniques used in the present work are discussed. Section 2.6 describes the photocatalysis technique using UV and sunlight. Biocompatibility is discussed in Section 2.7.

2.1 Sol-Gel Synthesis of TiO_2 and $Ti_{1-x}Mn_xO_2$ Nanoparticles

TiO_2 nanoparticles were synthesized using analytical grade $Ti(OC_3H_7)_4$ (titanium isopropoxide; Sigma Aldrich) as a precursor and C_2H_5OH (absolute ethanol; MERCK) as a solvent. A volume ratio of titanium isopropoxide and ethanol adjusted to 1:4. The mixture was kept for stirring till 1 h. Few drops of HNO_3 (MERCK) were added slowly to the solution as a stabilizer. The *p*H level was in the range from 6 to 6.5, measured using a digital *p*H meter. Water was added to initiate the hydrolysis process. After 5 to 10 minutes of stirring the sol was transferred to gel form. The obtained gel was kept 1 day for aging. Thereafter, the product was dried using a hot plate. Then the dried sample was crushed with the help of a mortar and pestle. At 500 ºC the sample was calcined

after crushing to obtain final product [Bharati et al. (2017)]. The experimental scheme for the synthesis of TiO_2 nanoparticles is illustrated in Figure 2.1. For Mn doped TiO_2 nanoparticles, manganese chloride ($MnCl_2$; HIMEDIA) solution was added to the titanium isopropoxide and ethanol solution then stirred for 1h to obtain uniform mixing before hydrolysis. The pH was maintained at 6.5. The concentration of Mn was calculated for 1, 2 and 3 at% with respect to TiO_2. The hydrolyzed samples were dried and calcined at 500 ºC to obtain the final products. Detailed scheme of synthesis for Mn doped TiO_2 is shown in Figure 2.2.

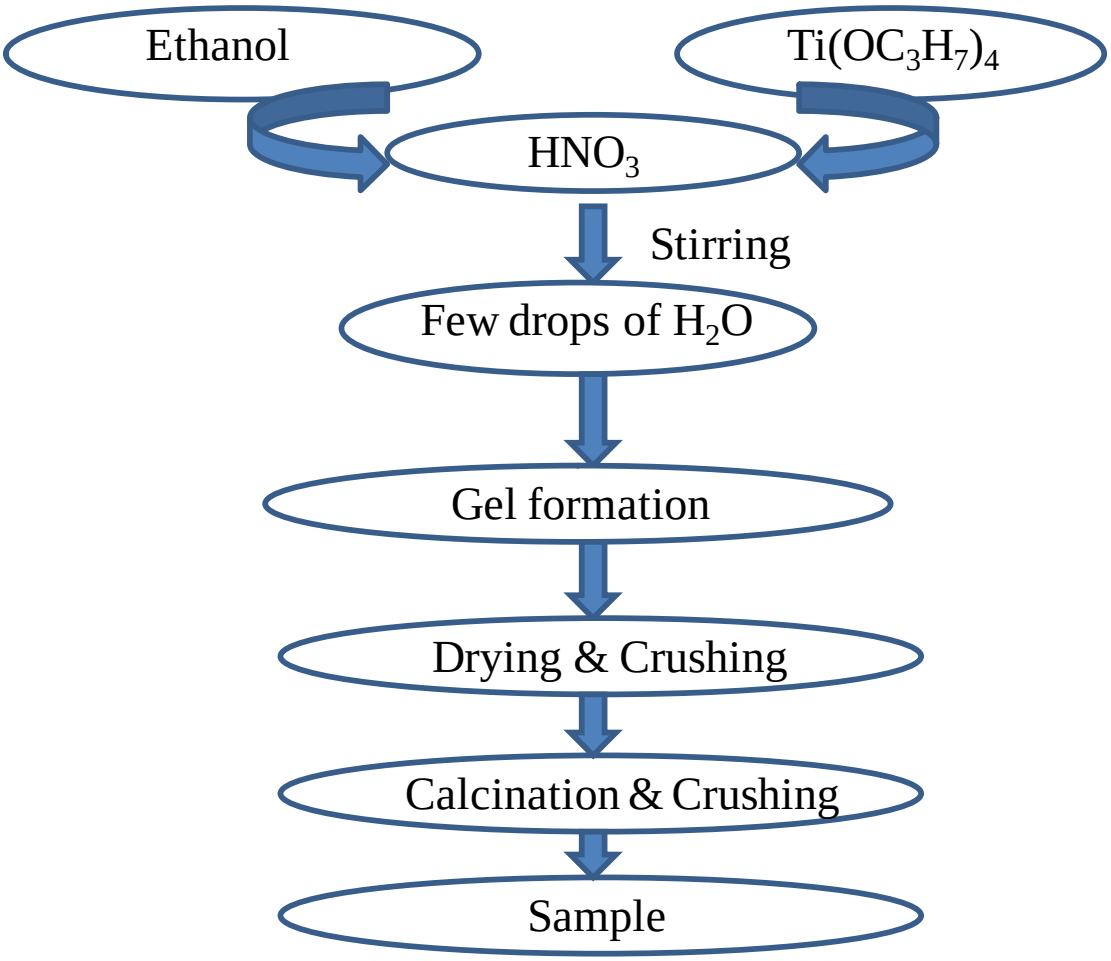

Figure 2.1 *Experimental scheme for synthesis of TiO_2 nanoparticles.*

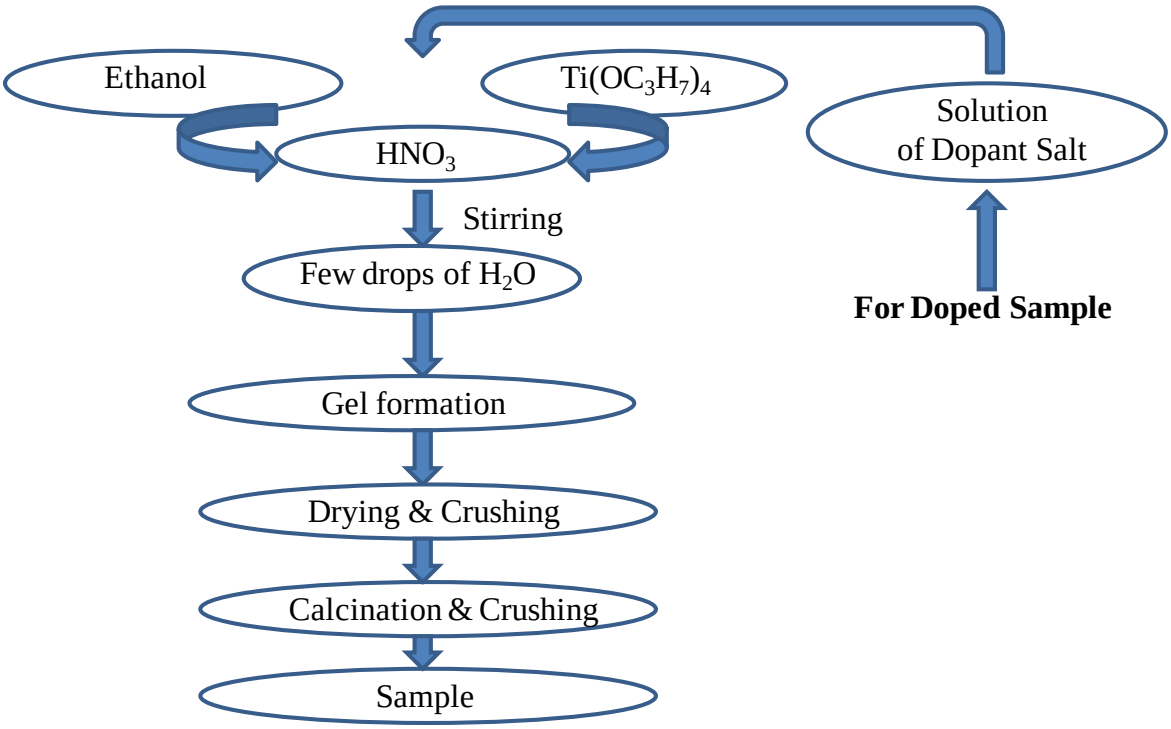

Figure 2.2 *Experimental scheme for the synthesis of Mn doped TiO_2 nanoparticles.*

2.2 Deposition of TiO_2 Thin Films by e-Beam Evaporation Technique

In e-beam evaporation technique, a stream of the electron beam is bombarded to the evaporant material kept in a vacuum chamber, therefore it attains the vapor pressure necessary for its evaporation. The stream of electrons is propagated through a potential difference of 5 to 10 kV and simultaneously focused magnetically onto the surface of the material to be evaporated. Electrons are lost their energy very rapidly after striking the surface of the material, and the material gets melt at the surface concurrently evaporates. The material is kept in a crucible with water-cooling support inside the chamber, by which the material remains solid which is in immediate contact with the crucible. Consequently, the crucible wall is coated with the target material and the molten material is present in that crucible is used for deposition, which controls the contamination in the film. Then the molten material gets evaporate and allowed to condense on a substrate

Figure 2.3 *Electron beam evaporation unit used for the deposition of TiO_2 film.*

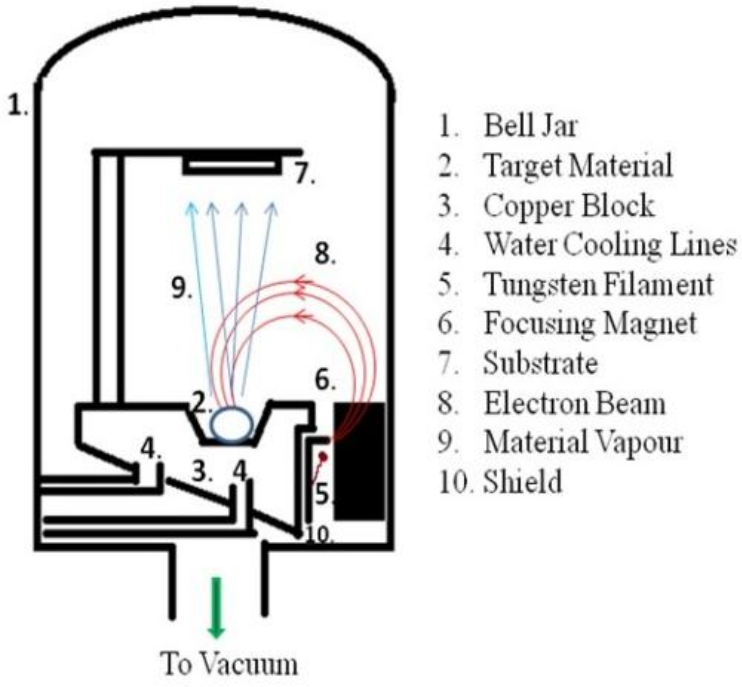

Figure 2.4 *The schematic diagram of the e-beam evaporation arrangement depicting various parts [Mohanty et al. (2014)a].*

kept at an appropriate distance. This e-beam evaporation technique is used for the deposition of TiO_2 film is shown in Figure 2.3 which is installed at IUAC, New Delhi. The various parts of the deposition chamber are sketched schematically in Figure 2.4.

The film thickness measurement was carried out by means of a quartz crystal monitor located in the deposition chamber. The distance inbetween the source to the substrate as well as to quartz crystal thickness monitor was 14 cm. After cleaning the Si (n-type <100>) substrates subsequently with boiled acetone and trichloroethylene (TCE), then with alcohol and distilled water, thereafter substrate is kept for drying. The dried substrate then mounted on a sample holder. To increase the vacuum level up to ~ 1.1 $\times 10^{-6}$ mbar, before deposition, liquid nitrogen was used inside the diffusion pump and pressure, ~ 4×10^{-5} mbar was maintained at the time of deposition. 20 mA current supplied to the electron gun was during deposition. The rate of deposition was limited to 0.2 nm/s. The target of high purity TiO_2 (99.99%, of STREM Chemicals, USA) was used for deposition [Bharati et al. (2018)a].

2.3 Fabrication of Pellets of TiO_2-Cement

In this work, we made the pellets with the help of plastic molds as shown in Figure 2.5 and the scheme of TiO_2-cement pellet preparation is shown in Figure 2.6.

To prepare composite pellets of TiO_2 and cement, first of all, we mix well both TiO_2 and cement and poured the mixture into the mold. After that little amount of water

Figure 2.5 *Pictorial representation of the fabrication of TiO_2-cement composite pellets.*

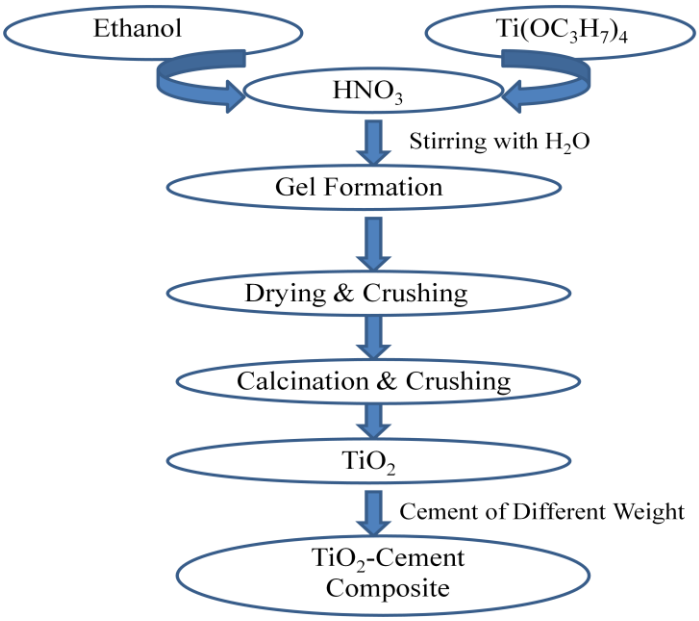

Figure 2.6 *Experimental scheme for the synthesis of TiO_2-Cement pellets.*

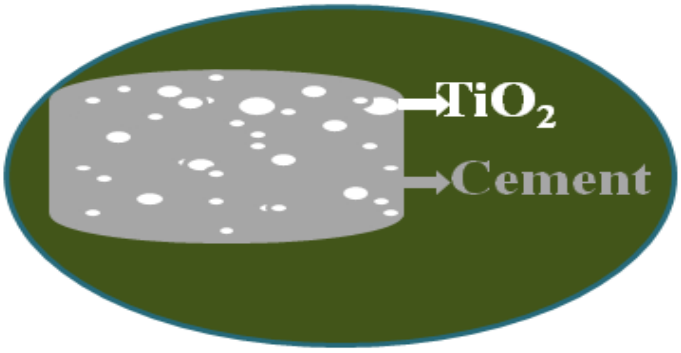

Figure 2.7 *The schematic diagram of cement and TiO_2 composite.*

was added dropwise to the mixture. Then kept the pellets in the air for two days, thereafter kept it in a container containing water for 10 days to strengthen the pellet. After removing the pellet from the water kept it in the air, 3 to 5 days for drying. The pellets are with three different compositions such as 50 mg TiO_2 and 20 mg cement and

referred as TC1, whereas pellets with 50 mg cement with 20 and 10 mg TiO_2 referred as TC2 and TC3, respectively. The schematic diagram of TiO_2-Cement composite pellet is shown in Figure 2.7.

2.4 Low Energy Ion Irradiation on TiO_2 Thin Films

The Electron Cyclotron Resonance Source

Inter-University Accelerator Centre (IUAC), New Delhi, supplies the low energy ion beam (LEIB). Ion beams having various charges with a wide range of energies inbetween keV to MeV, used for different experiments in Molecular, Atomic and Materials Science. The ion beam facility is having an Electron Cyclotron Resonance ion source and is placed on a high voltage floor. It is a kind facility which is made up of permanent magnet (NdFeB) design for axial as well as radial detention of plasma gives

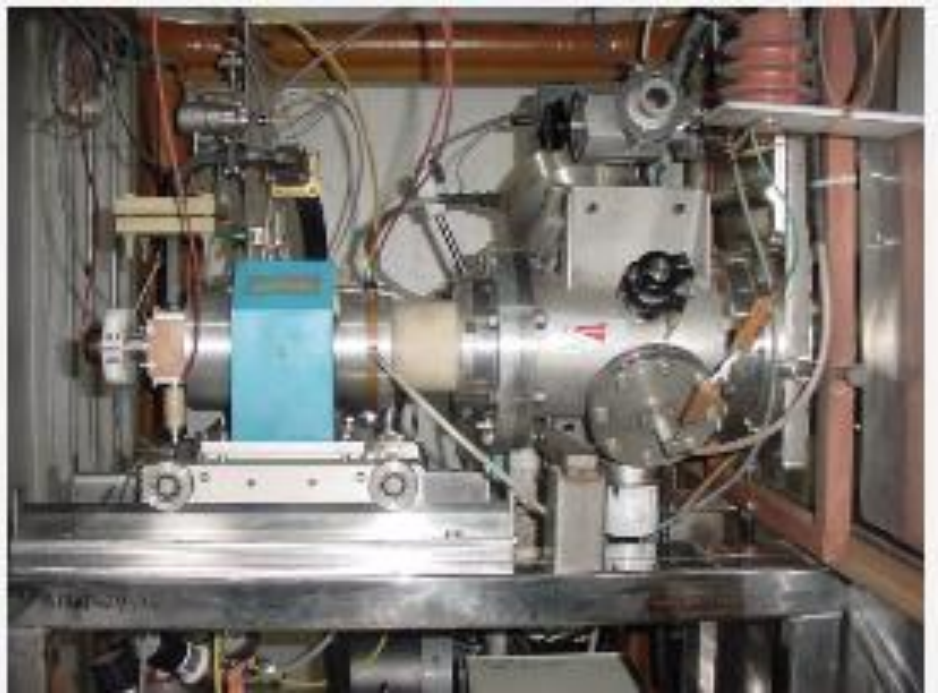

Figure 2.8 *ECR ion source used for low energy ion beam irradiation (IUAC).*

an outstanding prospect to perform research in atomic physics, materials and surface science. The UHF transmitter having high power (10 GHz) which is an electronic control device of the ECR source sited on a deck having high voltage. These ECR sources are constrained for using the multiplexed mode of optical fiber communication. Growth of platform having high voltage, beamlines in addition to machineries such as all metal double slit, electrostatic quadruple triplet lens, Faraday cups, beam steerers, UHV scattering chamber, all metal pneumatic straight through valve and the accelerating systems are made indigenously.

The ECR source of ion of IUAC placed on the deck having high voltage is revealed in Figure 2.8. LEIBF is a unique facility for different stimulating research works in the field of materials science, for example, epitaxial recrystallization induced by ion beams, modification of surface as well as properties at the near surface of the materials, interactions of solid surfaces and highly charged ions, doping of rare earth elements in semiconductors and nanostructure formations in semiconductors. The ion beams with the range of energies and charge states are depicted below in Table 2.1.

Table 2.1 *Different ions with their charge states and range of energy.*

Ion	Charge States	Energy Range
Oxygen	1+ to 6+	50 keV- 0.9 MeV
Argon	1+ to 10+	50 keV- 1.5 MeV
Xenon	1+ to 20+	50 keV- 3.0 MeV
Lead	1+ to 15+	50 keV- 2.2 MeV

We have irradiated 500 keV Ar^{2+} ions on the TiO_2 thin films which are present on Si substrate is grown through e-beam evaporation technique. The films were pasted on the ladder along its length vertically using double sided tape. The selected ion fluences were1 × 10^{14}, 5 × 10^{14}, 1 × 10^{15}, 5 × 10^{15}, 1 × 10^{16} and 5 × 10^{16} ions/cm^2 irradiated on TiO_2 thin films deposited on Si substrate [Bharati et al (2018)a,b].

2.5 Characterisation Techniques

The synthesized samples were characterized through different characterization techniques, such as XRD, Raman, XPS, BET, RBS and UV-Visible spectra. The details of characterization techniques are explained below.

2.5.1 X-Ray Diffraction (XRD)

XRD is a powerful method to investigate the purity as well as the crystal structure of the material. It also gives information regarding the crystallite size, the orientation of crystallites, strain, etc. A beam of X-rays, diffracted in different directions when it falls on a crystalline material of the definite structure. One can determine the crystal structure from XRD by measuring the intensities and angles of the diffracted beam. For a given inter-planer spacing of '*d*', the provision for diffraction to occur is given by Bragg's law i.e., $2d \sin\theta = n\lambda$, whereas, 'θ' is the angle between the surface of the sample and the incident X-ray, "*n*" is the integer, where the 'λ' is the wavelength of the incident radiation. The schematic diagram of Bragg's law is shown in Figure 2.9. In the case of thin films, where the thickness is practically very small, therefore, the intensity of the substrate is dominant. Thus, for thin films glancing angle mode XRD is preferable. In glancing angle mode X-rays, X-ray is incident on the surface of the film

through an extremely small angle (< 1º), which increase the path for the X-rays, and it is diffracted from the film surface without penetrating into the film.

In this work, a rotating anode of 18 kW (CuK_α), Rigaku powder diffractometer operating with the Bragg-Brentano geometry which is fixed with a monochromator of graphite in the diffracted beam was used to record the diffraction patterns for the powder samples. During the XRD measurements of the powder samples, the current was 100 mA and the voltage was 40 kV with 2θ ranging from 20 to 80º. Le Bail fittings of the XRD profiles were performed using FullProf software package. For thin films, advance X-ray diffractometer, Bruker D8 was used accompanied with a quick counting detector build on the Silicon strip technology. During the XRD measurements of the thin films, the current was kept 40 mA and voltage was 40 kV. The glancing angle was maintained at 0.5º with 2θ range from 20 to 50º.

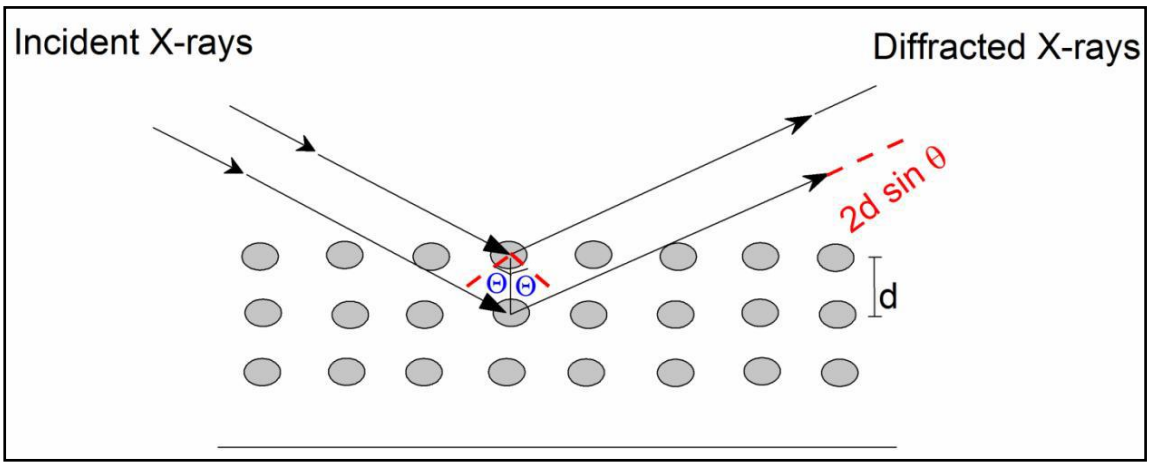

Figure 2.9 *Schematic representation of incident and diffracted X-rays from the crystal lattice.*

2.5.2 Raman Spectroscopy

A characterization technique, Raman spectroscopy is based on laser source, in this technique monochromatic light is scattered inelastic. After interacting the monochromatic light with the sample the frequency of these inelastic scattering of the photons are changes. In this the sample absorbes the photons from the laser light and re-emit it. The shifted frequency of the re-emitted photons goes up or down compared to the initial frequency of the monochromatic light which is commonly called as Raman effect. This Raman effect exhibits the information regarding rotational, vibrational as well as other low frequency transitions in molecules or solids, which gives the information about the structure of the material.

To find out the structure of the synthesised samples Raman spectrometers from JobinYvon Horiba (HR 800) and RENISHAW inVia using argon laser source ($\lambda \sim 488$ nm) were used for the current work. Raman spectra of the samples were recorded in between the 100 to 800 cm^{-1} range for both powder samples as well as for the thin films.

2.5.3 X-Ray Photoelectron Spectroscopy (XPS)

This technique is used for the analysis of the chemical state of the elements. This technique is sensitive at the surface which provides knowledge regarding the composition of the material and valence state of the elements constituting the material. Its principle is based on the photoelectric effect. When the sample is irradiated with the monochromatic X-ray photons having energy hν, emits electrons from the sample surface. The kinetic energy (K.E.) of emitted electrons is given by

$$K.E. = h\nu - B.E. - \Phi \quad \ldots\ldots\ldots\ldots\ldots\ldots (2.1)$$

Where ‘hν’ represents the energy of the incident X-ray photon, ‘B.E.’ represents the binding energy of the electron, where ‘Φ’ represents the work function. From equation

2.1, it is clear that photoelectrons can be produced only if $h\nu \geq B.E. + \Phi$. The emitted electrons are sorted by their K.E.

In the present study, we employed XPS instruments from VSW and AMICUS providing Al-K_α (energy = 1486.6 eV) and Mg-K_α (energy = 1253.6 eV) radiations, respectively. Vacuum level for sample preparation compartment (SPC) was ~ 10^{-8} Torr and the sample analysis chamber (SAC) was ~ 10^{-9} Torr. First of all, we scanned over the full energy range (survey scan), and then specifically selected Ti 2p, O 1s and Mn 2p core level spectra for our study. All observed peaks were calibrated to C 1s peak at 284.8 eV. XPS data were fitted using XPS peak 4.2 software.

2.5.4 Rutherford's Backscattering Spectrometry (RBS)

The fundamental importance of ion beam based characterization techniques is the awareness come from the slow down the ions when propagating in a material. Perception of the depth follows directly from the energy loss after probing the particles and the loss of energy affects both compositional and quantitative analysis. The science behind the loss of energy process is a complicated interaction between the ion, target electrons and the target nuclei. In backscattering spectrometry, for accurate determination of stoichiometry, impurity distributions and elemental density in thin films ion beams with MeV range energies have been extensively used. Ions to be analyzed are elastically scattered from the target atoms having characteristic energy related to the mass of the particle which strikes. They are loose energy during entering and exiting of the film. The energy of the backscattered ions is evaluated by the detection system which produces the spectrum of backscattering in the way of counts/channel to the channel number. The channel numbers are related linearly to the energy of the backscattered ions. A flat shaped peak appears for every element that exists in the sample. The peak width

appeared because of the energy loss in the ions present in the sample. Rutherford backscattering spectrometry (Pelletron Accelerator RBS-AMS Systems) facility has been installed at IUAC for characterization of materials. It is a non-destructive characterization tool used for accelerator based research laboratory having charge exchange radio frequency ion source producing negatively charged helium ions. 1.7 million volts tendem pelletron accelerator, analyzing magnet and target chamber equipped with goniometer, two surface barrier detector and one X-ray detector. Measurements are performed at resonant energies for oxygen, nitrogen and carbon. Surface barrier detector was used to measure the energy of the backscattered ions upon colliding with the atoms present in the sample which make us enable to find atomic mass along with elemental concentration and depth of the film below the surface.

Thin films of TiO_2 deposited on Si, were mounted on the sample holder using carbon tape. For calibration of the instrument, a gold film deposited on glass substrate was used. Sample positions were varied automatically using a goniometer controlled by a computer.

2.5.5 Transmission Electron Microscopy (TEM)

Transmission electron microscopy (TEM), takes high energy electrons to penetrate through a ($\leq$ 100 nm) sample. This offers increased spatial resolution in imaging (down to atomic scales) as well as the possibility of carrying out diffraction from nano-sized volumes. When the electrons are propagated up to the levels of high energy i.e. few hundreds keV and that is focused on the sample, they may either elastically or inelastically scatter, backscatter, or create many relations, which acts as the source for different signals such as Auger electrons, X-rays or light [Willams and Carter

(1996)]. To find out the size, shape of nanoparticles, we used a TEM from Tecnai G^2 20 Twin.

High Resolution Transmission Electron Microscopy (HRTEM), is the advance version of imaging in the TEM, provides the information at atomic scale level, with the image of the crystal structure of a sample. The scattered and transmitted beams are used to generate an interference image. The phase contrast picture of HRTEM is very small similar to the unit cell in the crystal. It can create high resolution images below 0.1 Å at magnification. The basic alignment of the TEM sample was orientation, rotation center, height, defocus, astigmatism, etc. The voltage applied for the electron gun is 200 kV. The well distinguished atomic planes of HRTEM were indexed by calculating the interplanar distance and were compared with the XRD data to confirm the phase.

Samples were prepared by dispersing 1 mg of powder in 10 ml of ethanol and sonicated in an ultrasonicator for homogeneous mixing. A drop of sonicated solution was cast on the commercial TEM grid (carbon coated copper grid). Further, the grid was dried to evaporate the volatile alcohol.

2.5.6 Scanning Electron Microscopy (SEM)

It is an essential tool to analyze the magnified images of insulating, semiconducting and metallic materials. It uses accelerated electrons instead of electromagnetic radiation to form an image. A stream of electrons is created by an electron gun and are moved from a few hundred eV to 40 keV. The beam of electron follows a path in the microscope appeared vertical, which is held in the high vacuum. The electron beam is focused on the sample surface using magnetic lenses to the mark which has a size of diameter in ~0.4 to 5 nm. When the beam hits the sample, X-rays and electrons are ejected from the surface of the sample. These secondary electrons,

backscattered electrons, X-rays are converted into the signals after collecting with the help of detectors and which can be visualized on a computer screen. The electron beam is scanned throughout the sample surface by means of magnetic scan coils. The current produced because of the backscattered electrons is collected and amplified then plotted as a 'micrograph' with a two-dimensional image. For SEM, samples should be conducting to ensure no charging during the measurement.

For the present study, a high resolution emission gun based scanning electron microscope (HR-SEM) (Zeiss, Germany), organized with the X-ray analyzer, was used. TiO_2 and Mn doped TiO_2 nanoparticles were mounted on the sample holder using carbon tape. The gun voltage was varied to capture well focused image of the sample.

2.5.7 Scanning Probe Microscopy (SPM)

This consists a group of techniques which evaluate the topography with their properties. Among them, we used AFM (Atomic Force Microscopy) to characterize the

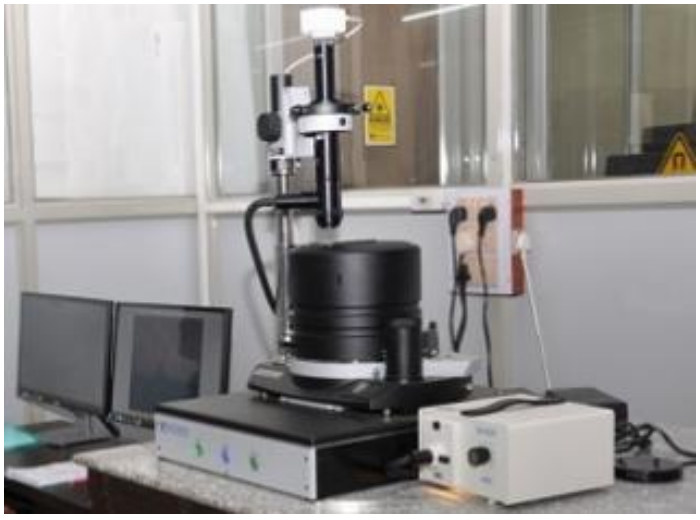

Figure 2.10 *Scanning Probe Microscope used for the analysis of the sample.*

thin films. An AFM consists of a cantilever with a pointed piezoelectric tip at the end which scans over the surface of the sample. The force among the tip and the sample directed a deflection in the cantilever when the tip approaches the sample surface. These deflections are measured with the laser spot which comes from the surface of the cantilever. The photodetector converts the difference in laser signals into a voltage that reconstructs the surface topography. Feedback from the computer maintains the tip either at a constant force or constant height above the sample surface.

AFM was done using SPM from NT-MDT Instruments. The images were obtained in SPM method with the help of the tip provided by NT-MDT. The Nova-Px software used for analyzing SPM image which was supplied by SPM Instruments installed at CIFC, IIT (BHU). SPM facility of IIT (BHU) is shown in Figure 2.10.

2.5.8 Brunauer-Emmett-Teller Measurement (BET)

The standard technique for finding the specific surface area of the sample is done by adsorption of gas. To estimate the surface area Brunauer, Emmett, and Teller (BET) equation is used. Barrett-Joyner-Halenda (BJH) analysis is used to determine the specific pore volume and pore area using a technique performed by adsorption and desorption of the gas. This technique provides both the porosity and pore size distribution of the sample. The parameters like size distribution of the pores, pore shape, particle size along with surface area act an important position in leading the very important reaction parameters like selectivity, stability and catalytic activity as well as physical factors such as diffusivity, mechanical strength, effectiveness factor and permeability. Therefore, to determine the porosity of the synthesized sample, in this work, we used micrometrics instrument.

In the present study, Brunauer-Emmett-Teller (BET) surface areas of Mn doped TiO_2 was measured at the temperature -196 ºC with the help of the Micromeritics ASAP 2020 Analyser. Under vacuum, the sample was degassed before the measurement at the temperature 300 ºC. Specific surface area of the sample was calculated using the data obtained from adsorption at the relative pressure (p/p_o) from 0.05 to 0.35. The sample pore size distribution was estimated from the isotherm curve of desorption using the BJH algorithm. The position of the maximum in the pore-size distribution was defined as pore diameter.

2.5.9 UV-Visible Spectroscopy

A spectrophotometer is an optical device, which transmits the specific band of electromagnetic spectrum appropriately selected with the help of diffraction (diffraction

Figure 2.11 *Shimadzu 2600 UV-Visible Spectrophotometer.*

grating) or by refraction (through a prism). The UV-Visible spectroscopy helps in finding out absorbance of the material. Materials of known absorbance or bandgap can simply be identified with the UV-visible spectroscopy. UV-Visible Spectrophotometer of Shimadzu Model 2600 used in this work is shown in Figure 2.11.

For the experiments, we used double beam spectrophotometers to record the absorbance of the samples (Shimadzu Model 2600). In a double beam spectrophotometer, for powder sample, one beam was incident on the sample and other one incident on the standard reference, $BaSO_4$ powder. For liquid samples reference was water. To record the spectra a photomultiplier tube (PMT) was used. For the UV light source, deuterium lamp was used and for visible light source, a tungsten lamp was used. Measurements of the powder samples were carried out in the diffused reflectance mode with the help of an integrating sphere assembly supplied with the Shimadzu 2600 spectrophotometer. Using the Kubelka-Munk function reflectance was converted to the absorbance.

2.5.10 Magnetic Measurements

The magnetic state of any material is determined by performing the magnetic measurements of the sample. The basic measurements help to get the magnetic behavior of the materials are i) measurement of magnetization as a function of temperature at the constant magnetic field and ii) measurement of magnetization versus applied external magnetic field at a constant temperature. In this work, we have used Magnetic Property Measurement System (SQUID-VSM, MPMS from Quantum Design, USA). This facility was installed at CIFC, IIT (BHU), India. Magnetic measurement facility, MPMS of IIT (BHU) is shown in Figure 2.12.

Figure 2.12 *Magnetic properties measurement system used for magnetic properties measurement.*

2.6 Photocatalysis under UV and Sunlight

In this work, photocatalytic behavior of the synthesized TiO_2 nanoparticles was evaluated under UV and sunlight by degrading the organic dyes, Methylene Blue (MB), Congo Red (CR) and Rhodamine B (RhB), as shown in Figure 2.13. In addition, the photocatalytic property of Mn doped TiO_2 samples was assessed under sunlight. To enhance the practical use of TiO_2 nanoparticles in environmental pollution control we carried out photocatalysis of TiO_2 with cement.

i) Photocatalysis using Powder Sample

The photocatalytic behavior of the prepared TiO_2 sample was estimated by the degradation of organic dyes in an aqueous solution such as MB, CR and RhB under UV and sunlight. By taking 5 mg of dye in one liter of distilled water the stock solution of the dyes was prepared. 50 ml of each dye solution was taken from the stock solution in the three different 50 ml conical flask and 20 mg of TiO_2 powder was added to the 50 ml dye solution present in the conical flasks. The prepared solutions of dyes and TiO_2 were kept for stirring in dark up to 30 min followed by exposer to 254 nm, UV light and natural sunlight at the day time, separately. At the particular intervals of time, ~3 to 4 ml of the light exposed dye and TiO_2 mixture was taken into the small glass vials. After that the absorbance was measured by using Shimadzu, UV-2600 UV-Visible spectrophotometer [Bharati et al (2017)].

ii) Photocatalysis using Pellet Sample

The photocatalytic activity of the prepared pellets of TiO_2 and cement was determined under sunlight through the degradation of aqueous organic impurity solutions, such as MB, CR and RhB. 50 ml of each dye solution with the pellets of TiO_2 and cement was taken in the 50 ml conical flasks, separately. Then the conical flask containing dye solution was kept for stirring in dark place up to 30 min, thereafter irradiated with sunlight. At particular intervals of time, ~ 3 to 4 ml of dye solution was taken from the irradiated solution and kept in the small glass vials. Further, the solution kept in glass vials is carried for absorbance measurement with the help of UV-Visible spectrophotometer (Shimadzu, UV-2600) [Bharati et al (2017)].

Figure 2.13 *Photocatalysis (a) under UV light and (b) under sunlight.*

iii) Degradation Percentage

Percentage of degradation of the dyes were calculated with the formula,

$$\text{Degradation \%} = \frac{Co-C}{Co} \times 100 \ldots\ldots\ldots\ldots\ldots\ldots (2.2)$$

Where, the C_o is the initial concentration of the dye solution and C is the concentration at time t [Bharati et al (2017)].

2.7 Biological Characterisation

2.7.1 Biocompatibility Study

Biocompatibility of the synthesized TiO_2 nanoparticles was examined through different biological tests, such as Platelet aggregation analysis, Hemolysis assay, MTT [(3-(4,5-Dimethylthiazol-2-yl)-2,5-Diphenyltetrazolium Bromide)] assay and Measurement of reactive oxygen species with TiO_2 nanoparticles [Bharati et al (2017)].

i) Platelet Preparation

From the clean human blood platelets were separated with the help of differential centrifugation. Blood picked from the healthy volunteers in citrate-phosphate-dextrose adenine then allowed for centrifuge at 180 g up to 20 min. Platelet-rich plasma (PRP) was incubated at the temperature 37 ºC up to 15 min with acetylsalicylic acid of the concentration 1 mM. The above sample of platelets was centrifuged at 800 g for 10 min after addition of 5 mM ethylene diamine tetraacetic acid (EDTA), and consequently, the platelets were sedimented. The sedimented platelets were washed in buffer A [20 mM HEPES, 138 mM NaCl, 2.9 mM KCl, 1 mM $MgCl_2$, 0.36 mM NaH_2PO_4, 1 mM EGTA (ethylene glycol tetra-acetic acid), supplemented with 5 mM glucose and 0.6 ADPase units of apyrase per ml, pH 6.2]. Lastly the in buffer B (pH 7.4), platelets were resuspended, where buffer B was the same as the buffer A, without apyrase and EGTA.

Finally, 0.5-0.8 × 10^9 per ml cell count was adjusted. Fluorescence microscope (Nikon model Eclipse Ti-E, Towa Optics, India) was used for morphology study of the cells with phase contrast attachment. Sterile conditions are maintained at every stage of the whole process and to keep the cells inactivate precautions were taken [Bharati et al (2017)].

ii) In Vitro Hemolysis Assay

From healthy human volunteers, fresh whole blood samples stabilized with EDTA were collected. For Red blood corpuscles (RBCs) separation, generally, 1 ml of fresh whole blood was mixed with 2 ml of phosphate buffer saline (PBS), then centrifuged for 10 min at 500 g. The separated RBCs are purified repeatedly four times. Afterward, the RBCs which are washed were diluted to 10 ml in PBS. TiO_2 in PBS was exposed to 1 ml of RBC suspension (~0.5 × 10^8 cells per ml) to examine its hemolytic activity. For obtain, the positive control RBCs were suspended in deionized water and for negative controls, it is suspended in PBS. Rocking shaker was used for sample incubation for 3 h at 37 ºC, followed by the centrifugation for 10 min at 10000 g. Hemoglobin absorbance was measured using micro plate spectrophotometer (BioTek model Power Wave XS2, Medispec India) at 540 nm, with 655 nm as the reference, at 37 ºC. Percent hemolysis was obtained using the equation given below [Bharati et al (2017)]:

$$\% \text{ Hemolysis} = \frac{\text{samples abs}_{540-655\text{nm}} - \text{negativecontrol abs}_{540\_655\text{nm}}}{\text{positivecontrol abs}_{540\_655\text{nm}} - \text{negativecontrol abs}_{540\_655\text{nm}}} \times 100 \ldots\ldots\ldots (2.3)$$

iii) Platelet Aggregation Studies

At 1200 rpm, for 1 min platelets were stirred at 37 ºC in a Whole Blood/Optical Lumi-Aggregometer (Chronolog model 700-2, Wheecon Instruments, India) before the addition of the TiO_2. Platelet aggregation was evaluated with the help of change in light transmission percent, in the blank sample, the transmittance is referred 100%. In the end, in Laemmlilysis buffer cells were boiled. Then stored at temperature -20 ºC for further analysis [Bharati et al (2017)].

iv) Measurement of Intracellular ROS

Oxidative activity of the platelets was determined using H_2DCF-DA, which is a ROS-sensitive probe. H_2DCF-DA was well known because of its diffusion into cells, by the intracellular esterases, its acetate groups were cleaved and simultaneously releasing the corresponding dichlorodihydrofluorescein (DCF) derivative. Subsequently, oxidation by the intracellular ROS produces a fluorescent adduct which was trapped within the cell. 20 μM H_2DCF-DA with the aliquots having platelet suspension (1×10^7 cells/ml) were incubated for 30 min at 37 ºC. Then after 20 min, TiO_2 was added to platelet suspensions. Fluorescence of the sample was measured at 37 ºC using the fluorescence micro plate reader (BioTek model FLx800, Medispec India) with the excitation, at 500 nm and emission, at 530 nm. As the positive control H_2O_2 (10 μM) was used in the platelet suspension [Bharati et al (2017)].

v) MTT Assay

The mitochondria of viable cells reduce tetrazolium component (MTT) into the insoluble dark-blue formazan product which is measured MTT assay. Cytotoxicity of TiO_2 nanoparticles was determined against platelets is found after the exposure of platelets with TiO_2 nanoparticles about 1 h. Then the cells were incubated along with 50

μM MTT at 37 ºC for 3 h. The produced formazan was soluble and dissolved in 200 μl of DMSO, next the absorbance was measured at 570 nm with the help of micro plate spectrophotometer (BioTek model Power Wave XS2, Medispec India) at 37 ºC. The processed culture was subjected to MTT assay as described in the cytotoxic estimation of TiO_2. Here, in this case, the untreated cells were taken as the positive control (100% viable) in the study [Bharati et al (2017)].

vi) Antibacterial MTT Assay

The quantitative assessment of antibacterial response on TiO_2 and Mn doped TiO_2 was performed using MTT (3(4, 5- dimethylthiazol-2-Yl)-2, 5-diphenyl tetrazolium bromide) assay. The S.Aureus (MTCC# 435) bacteria were procured in the freeze-dried condition from microbial type culture collection (MTCC) Chandigarh, India. The bacterial cells were cultured in their respective growth media (Nutrient Agar for S.Aureus) before seeding on the samples and incubated for 12 h at 37℃. The samples were seeded with 200 μl bacterial solution (with 0.1 optical density) per well in 24 tissue culture well plate and incubated at 37 ℃ for 8 h. After incubation, samples were washed with 1xPBS and reconstitute MTT (MTT: PBS in the ratio of 1:10) was mixed to the cultured samples then incubated for 2 h. MTT reacts with the viable cells and forms purple colored formazan crystal. These crystals were dissolved with dimethyl sulfoxide (DMSO). The absorbance of this formazan crystal was determined using ELISA micro plate reader (iMark Bio-red) at 595 nm. The absorbance of formazan crystal is proportional to the number of viable cells. The viability of bacterial cells was calculated as,

$$\% \text{ Viability } = \frac{\text{Mean absorbance of sample}}{\text{mean absorbance of uncharged HA}} \quad \ldots\ldots\ldots\ldots\ldots\ldots (2.4)$$

statistical analyses of the absorbance values were performed using SPSS software with one-way analysis of variance (ANOVA) method. Tukey test at significant value, $p < 0.05$ were performed for comparison of means.